Giant photocaloric effects across a vast temperature range in ferroelectric perovskites

Riccardo Rurali,[1] Carlos Escorihuela-Sayalero,[2,3] Josep Lluís Tamarit,[2,3] Jorge Íñiguez-González,[4,5] and Claudio Cazorla[2,3]

[1] *Institut de Ciència de Materials de Barcelona, ICMAB–CSIC, Campus UAB, 08193 Bellaterra, Spain*
[2] *Group of Characterization of Materials, Departament de Física, Universitat Politècnica de Catalunya, Campus Diagonal-Besòs, Av. Eduard Maristany 10–14, 08019 Barcelona, Spain*
[3] *Research Center in Multiscale Science and Engineering, Universitat Politècnica de Catalunya, Campus Diagonal-Besòs, Av. Eduard Maristany 10–14, 08019 Barcelona, Spain*
[4] *Luxembourg Institute of Science and Technology (LIST), Avenue des Hauts-Fourneaux 5, L-4362 Esch/Alzette, Luxembourg*
[5] *Department of Physics and Materials Science, University of Luxembourg, 41 Rue du Brill, L-4422 Belvaux, Luxembourg*

Solid-state cooling presents an energy-efficient and environmentally friendly alternative to traditional refrigeration technologies that rely on thermodynamic cycles involving greenhouse gases. However, conventional caloric effects face several challenges that impede their practical application in refrigeration devices. Firstly, operational temperature conditions must align closely with zero-field phase transition points; otherwise, the required driving fields become excessively large. But phase transitions occur infrequently near room temperature. Additionally, caloric effects typically exhibit strong temperature dependence and are sizeable only within relatively narrow temperature ranges. In this study, we employ first-principles simulation methods to demonstrate that light-driven phase transitions in polar oxide perovskites have the potential to overcome such limitations. Specifically, for the prototypical ferroelectric $KNbO_3$ we illustrate the existence of giant *photocaloric* effects induced by light absorption ($\Delta S_{\rm PC} \sim 100$ J K^{-1} kg^{-1} and $\Delta T_{\rm PC} \sim 10$ K) across a vast temperature range of several hundred Kelvin, encompassing room temperature. These findings are expected to be generalizable to other materials exhibiting similar polar behavior.

Solid-state cooling is an environmentally friendly and highly energy-efficient technology that harnesses caloric effects in materials for refrigeration purposes [1, 2]. Through the application of external fields to caloric materials, large reversible entropy and temperature changes ($\Delta S \sim$ 10–100 J K^{-1} kg^{-1} and $\Delta T \sim$ 1–10 K) can be achieved, seamlessly integrated into cooling cycles without reliance on greenhouse gases. Particularly, polar materials undergoing ferroelectric to paraelectric phase transitions under small electric fields are well-suited for solid-state cooling applications based on the electrocaloric (EC) effect [3–7], which can be miniaturized and coherently integrated into electronic circuits.

For caloric phenomena to be integrated in practical applications, the involved zero-field phase transition points must be close to room temperature. Otherwise, the necessary driving fields may reach impractically high levels, creating an energetically unfavorable scenario. Furthermore, the materials performance may suffer due to factors such as leakage/eddy currents, dielectric/magnetic losses, and mechanical fatigue. Unfortunately, only a limited number of compounds exhibit phase transitions near room temperature, which limits the range of solid-state refrigeration applications. Additionally, caloric effects typically exhibit strong temperature dependence and are substantial only within relatively narrow temperature ranges.

In this study, we propose a solution to the described caloric materials challenges by focusing on polar to non-polar phase transitions triggered by light absorption [8]. Specifically, we theoretically demonstrate the existence of giant *photocaloric* (PC) effects ($\Delta S_{\rm PC} \sim 100$ J K^{-1} kg^{-1} and $\Delta T_{\rm PC} \sim 10$ K) in the archetypal ferroelectric $KNbO_3$ (KNO). These PC effects persist across a vast temperature range spanning several hundred Kelvin, including room temperature, and are comparable to state-of-the-art EC effects [3–7]. The substantial anharmonicity of the paraelectric phase, naturally occurring at high temperatures ($\gtrsim 700$ K [9, 10]), coupled with its stabilization through light irradiation, are the primary factors responsible for the unravelled giant PC effects.

We performed density functional theory (DFT) calculations [11] with the projector augmented wave method [12] and generalized-gradient PBEsol approximation [13] (energy cutoff of 650 eV). The electrons treated as valence were: K $4s^1$ $3p^6$ $3s^2$, Nb $4d^4$ $5s^1$ $4p^6$, and O $2p^4$ $2s^2$. The first Brillouin zone (BZ) was sampled with a $12 \times 12 \times 12$ **k**-points grid and the atomic positions were optimized until the atomic forces were smaller than 0.5 meV Å^{-1}. Electric polarizations were calculated within a linear approximation using Born effective charges [14]. Photoexcitation was mimicked by constraining the partial occupancies of the electronic orbitals through adjustment of the Fermi distribution smearing. This effective DFT approach is effectively equivalent to those employed in previous works where the concentration of electron-hole pairs was constrained via the introduction of two adjustable quasi-Fermi levels [8, 15]. The second-order interatomic force constants were computed by finite differences with Phonopy [16] using $5 \times 5 \times 5$ su-

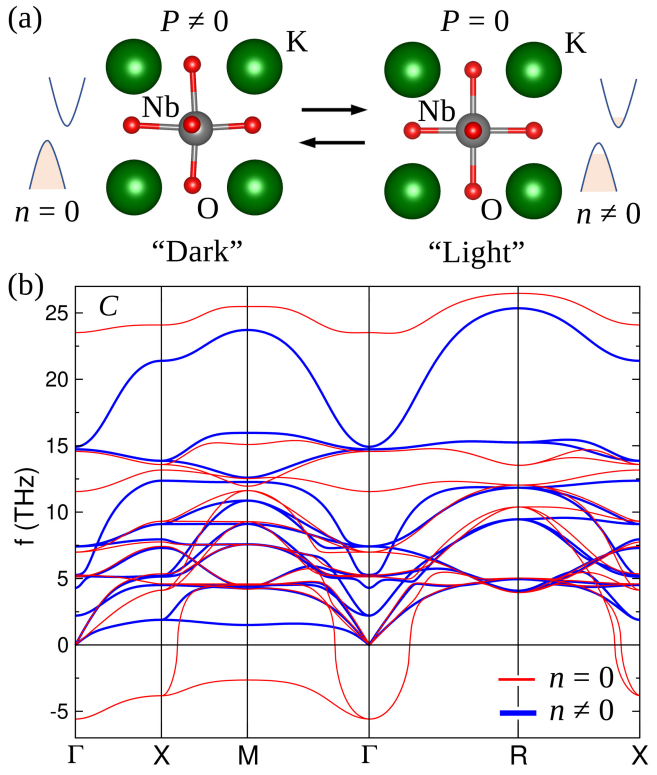

FIG. 1. **Light-driven phase transition mechanism in ferroelectric $KNbO_3$.** (a) Upon photoexcitation, electrons are promoted to the conduction band and ferroelectric KNO transforms into a nonpolar cubic phase, C. (b) Vibrational phonon spectrum of $KNbO_3$ in the nonpolar C phase at $T = 0$ K conditions in the absence (red lines) and presence (blue lines) of photoexcited electrons ($\overline{n} = 2.69 \cdot 10^{21}$ cm^{-3}).

percells for the polar phases and 4×4×4 supercells for the nonpolar phase. Thermal expansion effects were appropriately accounted for with the quasi-harmonic approximation (QHA) [17]. The DynaPhoPy code [18] was used to calculate the anharmonic lattice dynamics of the room-temperature polar phase (T-renormalized phonons) from *ab initio* molecular dynamics (AIMD) simulations. DFT Gibbs free energies, G, and entropies, S, were computed with the QHA method considering T-renormalized phonons for the phases that are dynamically unstable at zero-temperature conditions ("DFT-rQHA"). AIMD simulations were carried out in the (N, V, T) ensemble at $T = 300$ K using Nosé-Hoover thermostats. A large simulation cell containing $N = 625$ atoms was employed with periodic boundary conditions applied along the three Cartesian directions. Newton's equations of motion were integrated using the customary Verlet's algorithm with a time step of $1.5 \cdot 10^{-3}$ ps. Γ-point sampling was used for BZ integration and the total duration of the AIMD simulations was of 60 ps.

The ground state of KNO is a polar rhombohedral phase ($R3m$, R). At temperatures of $220 \leq T \leq 470$ K, KNO stabilizes in a different polar orthorhombic phase ($Amm2$, O) [9, 10]. Upon absorption of above-bandgap light, some electrons in KNO are photoexcited and promoted from the valence to the conduction band, where they gain increased mobility and become delocalized throughout the crystal. These carriers effectively screen the long-range dipole-dipole interactions that are key to the existence of polar order in the ferroelectric phase. Consequently, the nonpolar cubic phase ($Pm\overline{3}m$, C), which is stable at temperatures $T \gtrsim 700$ K under "dark" conditions [9, 10], becomes the ground state under "light" conditions (Fig. 1a).

Our zero-temperature DFT calculations reveal that the nonpolar C phase becomes vibrationally stable at photoexcited electronic densities exceeding $\overline{n} = 2.69 \cdot 10^{21}$ cm^{-3} (Fig. 1b). Importantly, our DFT simulations demonstrate that both the polar R and O phases spontaneously relax into the nonpolar C phase under sufficiently high light irradiation (or equivalently, density of photoexcited electron-hole pairs). Thus, under such photoexciting conditions the polar phases R and O are unstable rather than metastable. A similar light-induced phase transition has been shown to produce sizeable lattice thermal conductivity changes, with possible applications in energy scavenging and phonon-based logic [19].

In this study, above-bandgap light absorption is crucial since it drives the promotion of charge carriers from the valence to the conduction band. Hence, in practice the light frequency range should be in the ultraviolet region (i.e., $h\nu \geq E_g^{\mathrm{KNO}} \approx 3$ eV [20]). An essential parameter for the practical relevance of the described photoinduced phase-transition mechanism is the light penetration length, denoted as Δz. If Δz is too small, it could limit technological applications since the light-induced phase transition may not occur homogeneously unless $\Delta z \sim L$, where L represents a characteristic size of the sample. Based on experimental optical absorption data for KNO [20], we estimate $\Delta z \approx 30$ μm, which significantly exceeds the usual thickness of oxide perovskite thin films ($\sim$ 0.1–1.0 μm). Therefore, for practical implementations of the *photocaloric* phenomena revealed in this study, films are the most advisable systems.

According to our first-principles DFT calculations, the polar R phase is characterized by a lattice parameter of 4.034 Å, rhombohedral angle of 89.89° and ferroelectric polarization of $P = 35.05$ μC cm^{-2}. These results compare remarkably well with the corresponding experimental values ($T = 230$ K) of 4.016 Å, 89.83° and 30–40 μC cm^{-2}, respectively [9, 21, 22]. For the polar O phase, we estimated the unit cell parameters $a = 3.996$ Å, $b = c = 4.053$ Å, $\alpha = 90.18°$, and $\beta = \gamma = 90°$, and a ferroelectric polarization of $P = 38.53$ μC cm^{-2} along the pseudocubic direction [011]. These calculated values are also in very good agreement with the corresponding experimental results ($T = 295$ K) 3.973 Å, 4.035 Å, 90.27°, and ≈ 40 μC cm^{-2} [9, 21, 22]. Therefore, the employed DFT approach offers a robust description of KNO.

Figure 2 displays the vibrational phonon spectrum of the polar R and O phases at "dark" conditions. In the

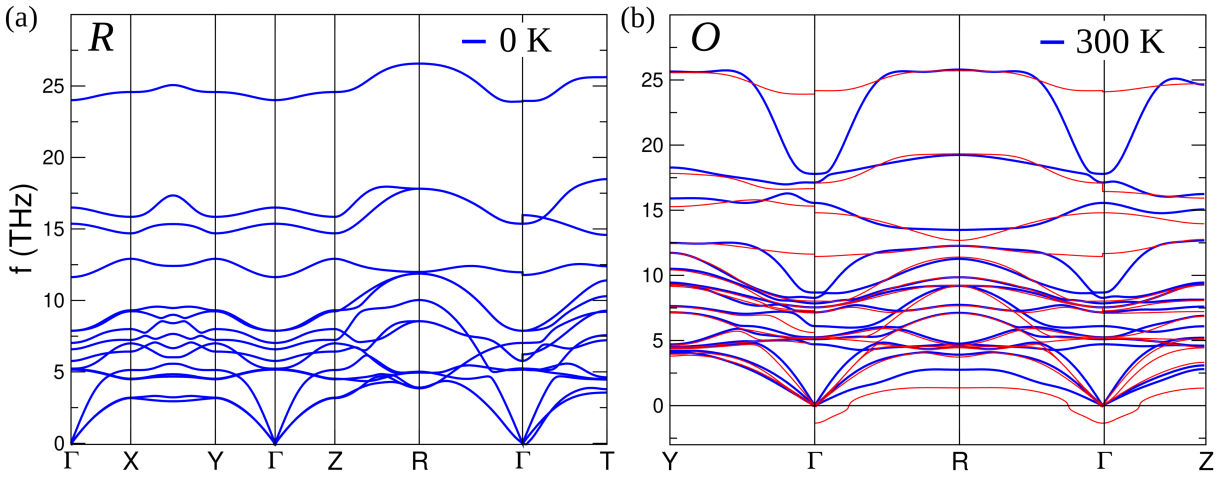

FIG. 2. **Phonon spectrum of $KNbO_3$ in the ferroelectric R and O phases at "dark" conditions.** The R phase is dynamically stable at zero temperature (a) whereas the O phase is not as shown by the thin red lines in (b). The T-renormalized phonon spectrum of the O phase renders dynamical stability around room temperature (blue lines) in agreement with the experimental observations [9, 10].

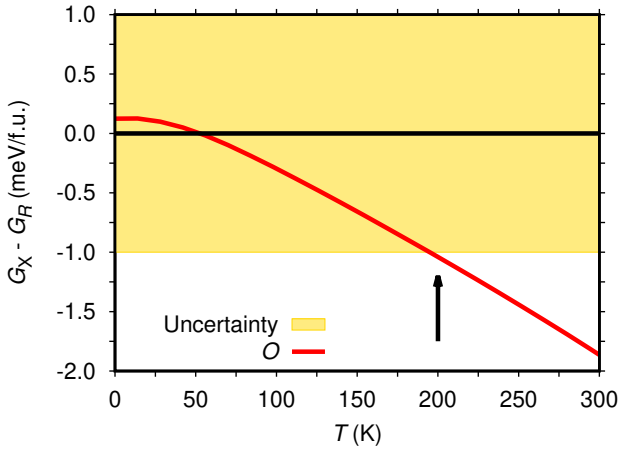

FIG. 3. **DFT-rQHA prediction of the T-induced $R \to O$ phase transition in $KNbO_3$.** The Gibbs free energy of the R and O phases cannot be distinguished in the temperature range $0 \leq T \lesssim 200$ K, taking into account the numerical uncertainties of 1 meV per formula unit. The polar O phase is predicted to become stable at temperatures $\gtrsim 200$ K (arrow) in fair agreement with the experiments [9, 10].

case of the O phase, the phonon frequencies were renormalized to account for thermal effects at room temperature using a normal-mode decomposition method [18]. Our computational results accurately replicate the dynamical stability observed in experiments for the polar R and O phases at low and room temperature, respectively [9, 10].

The Gibbs free energy (G) of the polar R and O phases was estimated with a numerical uncertainty of approximately 1 meV per formula unit (f.u.) as a function of temperature (i.e., based on the size of the employed supercells and other technical parameters), using the DFT-rQHA approach described earlier. These G functions enable the prediction of the temperature at which the phase transition $R \to O$ occurs, T_t, which is determined from the condition $G_O(T_t) = G_R(T_t)$. Figure 3 presents our DFT-rQHA Gibbs free energy results. We found that, considering the numerical uncertainties of 1 meV/f.u. and given the proximity in energy (near-degeneracy) of the two polymorphs, the Gibbs free energy of the R and O phases could not be distinguished in the temperature range $0 \leq T \lesssim 200$ K. However, at higher temperatures it is clearly appreciated that $G_O < G_R$. Consequently, from our calculations it can be assuredly concluded that the polar O phase becomes stable at temperatures above ≈ 200 K (Fig. 3), which is in reasonable agreement with the experimental transition temperature of 220 K [9, 10].

Subsequently, we computed the entropy, $S = -\partial G/\partial T$, of the R, O, and C phases as a function of temperature and light irradiation conditions, denoted as $S(T, x)$ (where $x = d, l$ stand for "dark" and "light" conditions, respectively). The resulting $S(T, x)$ curves exhibit smooth behavior, as explicitly shown in Fig. 4. Analogous to quasi-direct calorimetry experiments [23–25], the determination of the *photocaloric* isothermal entropy, $\Delta S_{\rm PC}$, and adiabatic temperature changes, $\Delta T_{\rm PC}$, can be readily inferred from these entropy curves [26]. In particular, we have that $\Delta S_{\rm PC} = S(T, l) - S(T, d)$ and $\Delta T_{\rm PC} = T_0(S, l) - T(S, d)$, where T_0 fulfills the condition $S(T_0, l) = S(T, d)$ (black solid lines in Fig. 4). We recall that under sufficiently high light irradiation (or equivalently, for photoexcited electronic densities $\geq \overline{n} = 2.69{\cdot}10^{21}$ cm^{-3}) the polar R and O phases spontaneously relax into the nonpolar C phase.

Figure 4 encloses examples of our evaluations for $\Delta S_{\rm PC}$ and $\Delta T_{\rm PC}$, considering different temperature intervals in which the polar R and O phases are observed to be thermodynamically stable. For instance, at a temperature of

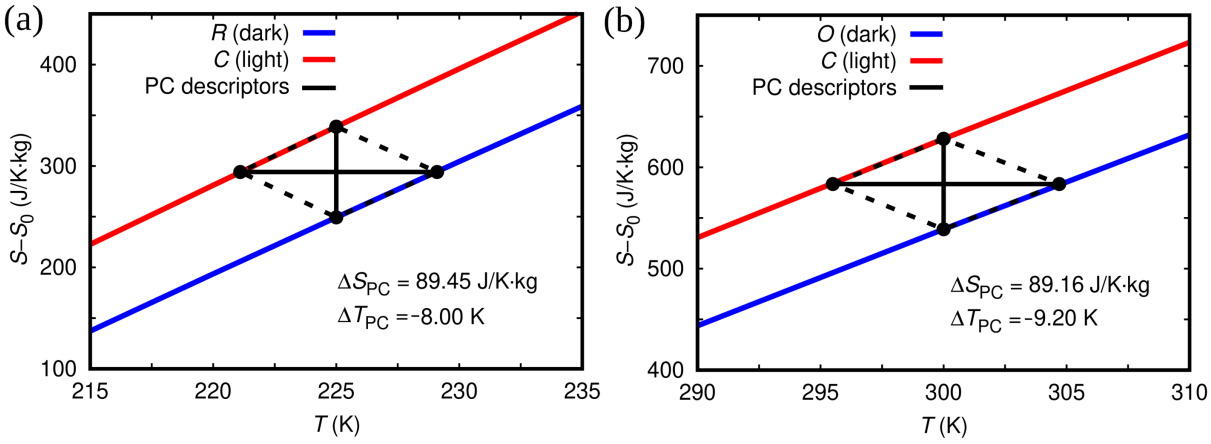

FIG. 4. **Evaluation of photocaloric effects in $KNbO_3$.** (a) At low temperatures, for the polar R (dark) and nonpolar C (light) phases. (b) Around room-temperature, for the polar O (dark) and nonpolar C (light) phases. ΔS_{PC} and ΔT_{PC} can be straightforwardly determined from the shown entropy curves (black solid lines) as done in quasi-direct calorimetry experiments [23–25]. "Light" conditions correspond to a photoexcited electronic density of $\overline{n} = 2.69 \cdot 10^{21}$ cm^{-3}.

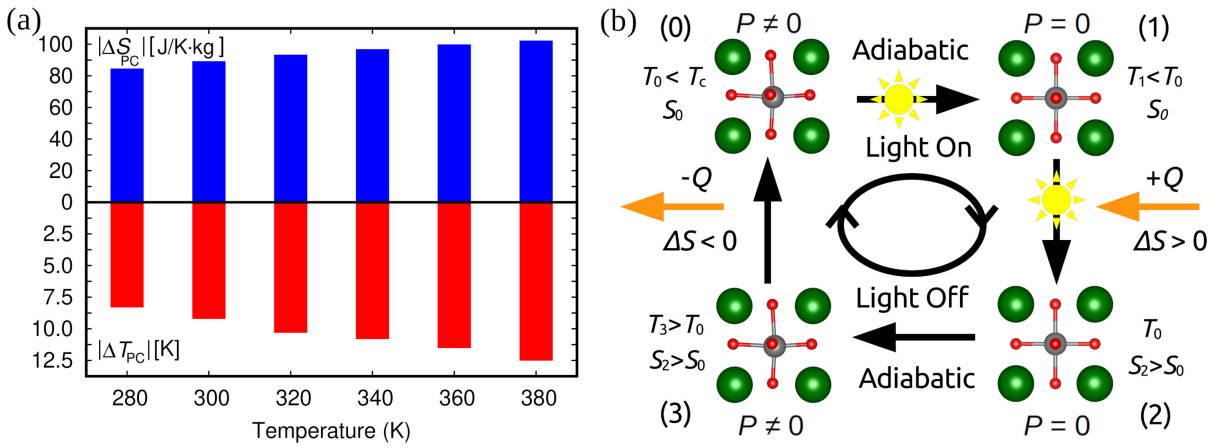

FIG. 5. **Extremely ample photocaloric operation conditions and envisaged solid-state refrigeration cycle.** (a) The magnitude of the two *photocaloric* descriptors $|\Delta S_{PC}|$ and $|\Delta T_{PC}|$ evaluated for $KNbO_3$ as a function of temperature. (b) A possible four-step solid-state refrigeration cycle based on the *photocaloric* effect unveiled in this study.

≈ 220 K and considering the R phase under dark conditions, we estimated a giant isothermal entropy change of 89.5 J K^{-1} kg^{-1} and an adiabatic temperature change of -8.0 K ($\Delta T_{PC} < 0$ since the state stabilized with light has higher entropy). Similarly, at room temperature and considering the O phase under dark conditions, we computed a substantial isothermal entropy change of 89.2 J K^{-1} kg^{-1} and an adiabatic temperature change of -9.2 K. These *photocaloric* results are highly promising for technological applications as they are comparable in magnitude to those obtained from state-of-the-art electrocaloric (EC) effects [3–7]. Furthermore, the magnitude of the $|\Delta T_{PC}|$ predicted for KNO is approximately one order of magnitude larger than the EC adiabatic temperature changes measured for similar polar materials such as $BaTiO_3$ (BTO) [27]. The relatively large $|\Delta T_{PC}|$ as compared to $|\Delta T_{EC}|$ (or equivalently, $|\Delta S_{PC}| > |\Delta S_{EC}|$) can be attributed to the unique nature of the light-induced phase transition: the nonpolar C state is directly stabilized, bypassing the intermediate polar states that are typically encountered during conventional T-induced transformations [9, 10]. Consequently, polar materials similar to KNO and presenting high Curie temperatures are probably most suitable for achieving substantial *photocaloric* responses.

A highly promising aspect of the *photocaloric* effect theoretically unveiled in this study, which sets it apart from other known caloric effects, is its operability over vast temperature intervals defined by the ranges of thermodynamic stability of the polar phases of the material. This exceptional characteristic is explicitly demonstrated in Fig. 5a, where we represent the values of the $|\Delta S_{PC}|$ and $|\Delta T_{PC}|$ estimated for KNO over an unprecendented wide temperature range spanning more than a hundred Kelvin, encompassing room temperature. Interestingly, both the isothermal entropy and adiabatic tem-

perature changes slightly but steadily increase with increasing temperature. For example, at $T = 380$ K, these quantities amount to 102.2 J K^{-1} kg^{-1} and 12.50 K, respectively. This behavior arises from the fact that the variation of the entropy upon increasing temperature, or equivalently the heat capacity $C_v = \frac{1}{T}(\partial S/\partial T)_V$, is somewhat higher for the nonpolar C phase than for the polar O phase (Fig. 4). The likely persistence of PC effects at very low temperatures makes the proposed scheme an appealing alternative for achieving cryogenic temperatures, which can be particularly useful in applications such as quantum computing. This possibility warrants future detailed theoretical exploration due to the inevitable consideration of quantum nuclear effects [17].

A possible four-step refrigeration cycle based on the *photocaloric* effect observed in KNO is envisioned (Fig. 5b). (0) $\rightarrow$ (1) *Adiabatic light exposure:* Initially, starting from the polar low-entropy O phase at room temperature, T_0, the KNO system is adiabatically irradiated until stabilizing the nonpolar high-entropy C phase. As a result, the temperature of the KNO sample decreases, $T_1 < T_0$ ($\Delta T_{\rm PC} < 0$). (1) $\rightarrow$ (2) *Heat transfer:* With the light conditions maintained, the KNO sample is placed in contact with the targeted body to be refrigerated, facilitating the transfer of heat towards KNO, $|Q| = T \cdot |\Delta S_{\rm PC}|$, until restoring its initial temperature conditions, $T_2 = T_0$. (2) $\rightarrow$ (3) *Adiabatic light removal:* The light is adiabatically switched off, stabilizing the polar low-entropy O phase again. Consequently, the temperature of the KNO sample increases, $T_3 > T_0$. (3) $\rightarrow$ (0) *Heat removal:* Finally, the KNO sample is placed in contact with a heat sink, allowing heat to flow from KNO until restoring the initial temperature conditions, thereby completing a cooling cycle.

In conclusion, we have presented compelling theoretical evidence for the existence of giant *photocaloric* effects driven by light absorption in the archetypal ferroelectric perovskite $KNbO_3$. The magnitude of the unveiled *photocaloric* effects is remarkably large, that is, comparable to the most promising electrocaloric effects measured in ferroelectrics. An unparalleled and distinctive feature of these *photocaloric* effects is that they remain very large over vast temperature intervals spanning several hundred Kelvin, only limited by the ranges of thermodynamic stability of the polar phases of the material. Therefore, this study provides motivation for exploring new concepts and strategies to develop environmentally friendly and highly miniaturizable solid-state cooling technologies.

ACKNOWLEDGEMENTS

We acknowledge financial support by the Spanish Ministry of Science under the grants PID2020-119777GB-I00, TED2021-130265B-C22, PID2020-112975GB-I00, RYC2018-024947-I and CEX2019-000917-S, and by the Generalitat de Catalunya under the grants 2021SGR-00343 and 2021SGR-01519. Computational support was provided by the Red Española de Supercomputación under the grants FI2022-1-0006, FI-2022-2-0003 and FI-2022-3-0014. We thank J. Carrete for useful discussions.

[1] X. Moya and N. D. Mathur, Science **370**, 797 (2020).
[2] L. Mañosa, A. Planes, Adv. Mater. **29**, 1603607 (2017).
[3] E. Defay, R. Faye, G. Despesse *et al.*, Nat. Commun. **9**, 1827 (2018).
[4] Y. Nouchokgwe, P. Lheritier, Ch. Hong *et al.*, Nat. Commun. **12**, 3298 (2021).
[5] S. E. Shirsath, C. Cazorla, T. Lu *et al.*, Nano Lett. **20**, 1262 (2020).
[6] C. Menéndez, R. Rurali and C. Cazorla, Phys. Chem. Chem. Phys. **25**, 17450 (2023).
[7] J. Li, A. Torelló, V. Kovakova *et al.*, Science **382**, 801 (2023).
[8] C. Paillard, E. Torun, L. Wirtz, J. Íñiguez and L. Bellaiche, Phys. Rev. Lett. **123**, 087601 (2019).
[9] D. Wang, G. Wang, Z. Lu *et al.*, Front. Mater. **7**, 91 (2020).
[10] G. Shirane, R. Newnham and R. Pepinsky, Phys. Rev. **96**, 581 (1954).
[11] G. Kresse and J. Furthmüller, Phys. Rev. B **54**, 11169 (1996).
[12] P. E. Blöchl, Phys. Rev. B **50**, 17953 (1994).
[13] J. P. Perdew, A. Ruzsinszky, G. I. Csonka *et al.*, Phys. Rev. Lett. **100**, 136406 (2008).
[14] C. Menéndez and C. Cazorla, Phys. Rev. Lett. **125**, 17601 (2020).
[15] B. Peng, Y. Hu, S. Murakami *et al.*, Sci. Adv. **6**, eabd1618 (2020).
[16] A. Togo and I. Tanaka, Scr. Mater **108**, 1 (2015)
[17] C. Cazorla and J. Boronat, Rev. Mod. Phys. **89**, 035003 (2017).
[18] A. Carreras, A. Togo and I. Tanaka, Comput. Phys. Commun. **221**, 221 (2017).
[19] C. Cazorla, S. Bichelmaier, C. Escorihuela-Sayalero *et al.*, Nanoscale DOI:10.1039/D4NR00100A (2024).
[20] Y. Kaifu, T. Komatsu, T. Hirano *et al.*, J. Phys. Soc. Jpn. **23**, 903 (1967).
[21] A. I. Frenkel, F. M. Wang, S. Kelly *et al.*, Phys. Rev. B **56**, 10869 (1997).
[22] M. D. Fontana, G. Metrat, J. L. Servoin *et al.*, J. Phys. C: Solid State Phys. **17**, 483 (1984).
[23] P. Lloveras, A. Aznar, M. Barrio *et al.*, Nat. Commun. **10**, 1803 (2019).
[24] A. Aznar, P. Lloveras, M. Barrio *et al.*, J. Mater. Chem. A **8**, 639 (2020).
[25] A. Aznar, P. Negrier, A. Planes *et al.*, Appl. Mater. Today **23**, 101023 (2021).
[26] C. Escorihuela-Sayalero, L. C. Pardo, M. Romanini *et al.*, npj Comput. Mater. **10**, 13 (2024).
[27] F. Han, Y. Bai, L.-J, Qiao *et al.*, J. Chem. Mater. C **4**, 1842 (2016).